Original Article

Possible Therapeutic Effect of Chitosan Nanoparticles versus Pioglitazone Loaded Chitosan Nanoparticles on Colitis Associated with Chronic Kidney Disease in Adult Male Albino Rat Model. Histological and Biochemical Study

Rokia Mohamad Hassan, Safinaz Salah Eldin Sayed, Alaa Serag El-dean Habib and Marwa Mohamed Yousry

Department of Histology, Faculty of Medicine, Cairo University, Cairo, Egypt

ABSTRACT

Background: One of the pathogenic factors and a complication of chronic kidney disease (CKD) is colitis and intestinal dysbiosis. Pioglitazone hydrochloride (PIO), an antidiabetic medication which stimulates peroxisome proliferator-activated receptor-γ (PPAR-γ) & possess antioxidant and anti-inflammatory effects. Low aqueous solubility of PIO results in limited absorption and pharmacodynamics. Therefore, a drug delivery system nanoparticle is a priority.

Aim of Work: Assessing the potential therapeutic impact of chitosan nanoparticles versus PIO-loaded chitosan nanoparticles on colitis associated with CKD.

Materials & Methods: Twenty-nine adult male rats were categorized into 5 groups: group I, group II administered adenine daily for 3 weeks, group III treated as group II then no further intervention for 2 weeks, groups IV & V received adenine as group II then treated with chitosan nanoparticles and PIO-loaded chitosan nanoparticles respectively for 2 weeks. Biochemical analysis for stool lactobacilli, serum creatinine, colonic malondialdehyde (MDA), tumor necrosis factor-α (TNF-α) and PPAR-γ along with histological and immunohistochemical study (for claudin-1 and caspase-3) were performed. In addition to statistical analysis.

Results: Group II illustrated elevated serum creatinine, colonic MDA and TNF-α as well as decreased stool lactobacilli and PPAR-γ expression. Disruption of renal architecture along with lost colonic surface epithelium, distorted intestinal crypt and inflammatory infiltration were recorded. In addition to reduced claudin-1 and increased caspase-3 immunoreactivity. As regards group III, no significant improvement was recorded in all the previously mentioned findings. While groups IV and V revealed obvious amelioration with better effects in group V.

Conclusion: Both chitosan nanoparticles and pioglitazone loaded chitosan nanoparticles improved alteration of kidney function and structure and ameliorated colitis associated with CKD. While pioglitazone loaded chitosan nanoparticles illustrated superior impacts.

Received: 23 May 2024, **Accepted:** 10 June 2024

Key Words: Chronic kidney disease induced colitis, claudin-1, intestinal microbiota, pioglitazone chitosan nanoparticles, PPAR-γ.

Corresponding Author: Marwa Mohamed Yousry, MD, Department of Histology, Faculty of Medicine, Cairo University, Cairo, Egypt, **Tel.**: +20 10 0676 3862, **E-mail:** marwa.yousry@kasralainy.edu.eg

ISSN: 1110-0559, Vol. 48, No. 2

INTRODUCTION

Chronic kidney disease (CKD), a common health issue, influences 9.1% of the population[1]. In CKD there is aberration in renal function or structure lasting more than three months irrespective of the cause[2]. The progression of renal dysfunction is associated with impaired structure and function of diversity organs and systems, as gastrointestinal tract[3].

In CKD, decline of the kidney function leads to improper clearing of uremic toxins resulting in increasing their load in the intestinal lumen. Gut microbiota act on these toxins & potentially produce detrimental byproducts to intestinal mucosa[3]. Many medications such as anti-inflammatory drugs, antibiotics and antihypertensive drugs are used in CKD patients, these drugs are also known to affect intestinal tract[4].

All the above-mentioned factors act together and cause dysbiosis, an imbalance in the intestinal microbiota (decrease in beneficial bacterial species and proliferation of harmful bacteria). This results in high levels of uremic toxins as indoxyl sulfate and p-cresol which compromise tight junctions between mucosal epithelial cells with subsequent increase in intestinal permeability. Impaired intestinal barrier leads to translocation of bacteria products and toxins into the systemic circulation. This contributes to the systemic inflammatory reaction & oxidative stress that have a key role in CKD progression which in turn increases the uremic toxins forming a vicious circle[5].

Nanoparticles are molecules with nano size[6]. This small size harbors many advantages as high surface to volume ratio, increased solubility and bioavailability, increased stability, elevated safety and efficacy[7].

DOI: 10.21608/ejh.2024.291579.2070

Chitosan is a natural derived mucopolysaccharide formed of N-acetylglucosamine and D-glucosamine[8]. Chitosan is frequently applied as a drug delivery system in oral route. This is owed to its many convenient properties such as mucoadhesion, controlled drug release, enhancement of absorption and biodegradability[9].

Pioglitazone is an anti-diabetic medication. It belongs to the thiazolidinedione (TZDs) family of drugs which is also known as glitazones. It acts as an insulin sensitizing drugs for treatment of type 2 diabetes[10]. Its action is mediated through its effect on peroxisome proliferator activated receptor-gamma (PPAR-γ)[11].

Expression of PPAR-γ is detected in epithelial cells throughout the intestine, predominate in distal colon[12]. It possesses anti-inflammatory impacts via inhibition of the nuclear factor kappa B (NF-κB) and expressions of inflammatory factors, tumor necrotic factor alpha (TNF-α) as well as interleukin-1 (IL-1). However, PPAR-γ was reduced and NF-κB expression was enhanced in the colonic mucosa of colitis individuals[13,14]. This finding justified the curiosity about the role of PPAR-γ in colitis as a probable therapeutic target.

AIM OF THE WORK

The current work aimed at evaluating the probable therapeutic impact of chitosan nanoparticles versus pioglitazone loaded chitosan nanoparticles on colitis secondary to adenine induced CKD in adult male rats.

MATERIALS & METHODS

Materials

Adenine sulphate was purchased from Lab chemicals trading co. (Cairo, Egypt). The drug, in the form of powder, was prepared freshly every day by dissolving each 1gm in 25 ml tap water[15].

Pioglitazone hydrochloride (PIO) was gifted by Averroes Pharma (Sadat city, Egypt) in the form of powder.

Chitosan NPs (CS NPs) with 85% degree of deacetylation (DD) was prepared by Nanogate company (Cairo, Egypt). Deacetylation is a process of removal of acetyl groups from chitin, leaving many amino groups in chitin molecules. The DD is a major factor which identifies some chemical as well as biological characteristics of chitosan[16].

Chitosan NPs (CS NPs) and pioglitazone loaded chitosan NPs (PIO-CS NPs) were prepared by Nanogate firm by ionic gelation technique which includes crosslinking of cationic chitosan amino groups to a polyanionic linker. Nanoparticles were provided in distilled water[17,18].

Experimental design

This study included twenty-nine male albino rats of ~200 grams weight and aged 10-12 weeks. Rats were purchased and raised in the Animal House of Faculty of Medicine, Cairo University. Animals lived in separate cages at 24 ± 1°C, fed standardized chow as well as water ad libitum. The present study was conducted according to ethical procedures & policies of the Animal Ethical Committee of Cairo University, (approval number, CU III F 22 21). The animals were classified into 5 groups.

Group I (Control group): It included nine animals which were further classified into three subgroups:

- Subgroup IA (3 rats): Each animal was administered 1ml tap water via intra-gastric tube once daily for three weeks then the rats were euthanized (corresponding to model group).
- Subgroup IB (3 rats): Rats were treated as subgroup IA. Then no further treatment was received for two weeks (corresponding to recovery group).
- Subgroup IC (3 rats): Rats were treated as subgroup IA. Then 1 ml distilled water was administered once every day for 2 weeks by intragastric tube (corresponding to NP groups).

Group II (CKD model group / 5 rats): Chronic kidney disease was conducted by oral treatment with adenine sulphate 200 mg/kg per day (each rat received 40mg of the drug solubilized in 1 ml tap water) for three weeks[15]. All rats of this group were euthanized at the end of three weeks to assess the establishment of chronic kidney disease.

Group III (Recovery group / 5 rats): Chronic kidney disease was conducted as group II then the rats were left without any further treatment and were euthanized after 2 weeks to evaluate spontaneous recovery.

Group IV (CS NPs group / 5 rats): Chronic kidney disease was conducted such as CKD model group. Then each rat was administered CS NPs with a dose of 120 mg/kg body weight corresponding to the mentioned ratio of the loaded NPs in group V[18]. The drug was solubilized in distilled water (1 ml) and orally administered by an intra-gastric tube, once daily till scarification after 2 weeks.

Group V (PIO-CS NPs group / 5 rats): Chronic kidney disease was conducted as in group II. Then each rat received PIO 15 mg /kg body weight[19] loaded on CS NPs 120 mg/kg body weight with a drug to chitosan carrier ratio of 1:8 corresponding to the dosing formula ratio of Borkhataria and Patel study[18]. The PIO-CS NPs was dissolved in 1 ml distilled water and administered once daily through intra-gastric tube till scarification after 2 weeks[19].

Methods

Nanoparticles studies

The loading capacity and encapsulation efficiency of PIO-CS NPs were calculated by Nanogate firm according to a previously described methodology[20]. The loading capacity and encapsulation efficiency were 11.05 % and 88.38 % respectively.

Animal studies

Faecal Study

At the end of experimental durations (three and five weeks), faecal samples from each rat of all groups were collected for DNA sequencing of faecal microbes for lactobacilli. Polymerase chain reaction (PCR) for lactobacilli DNA sequencing was done using QIAamp® Fast DNA Stool Mini Kit Protocol (catalogue no. 51604, Hilden, Germany). Primer sets for lactobacilli species were: F:5′- AGCAGTAGGGAATCTTCCA - 3′ R: 5′- CACCGCTACACATGGAG -3′ and GAPDH: F: 5'-TGGCATTGTGGAAGGGCTCA-3' R: 5'TGGATGCAGGGATGATGTTCT-3'.

Serological Study

Blood was collected from the rats' tail vein before euthanasia (three and five weeks) for evaluation of serum levels of creatinine to assess the functional state of kidney. Serum creatinine levels were measured using BioMed® Creatinine assay colorimetry kit (Hannover, Germany).

Specimen Collection and Processing

After termination of experiment durations, the rats of all experimental and control groups were injected intraperitoneally by anesthetic sodium pentobarbital (120 mg/kg)[21]. The right kidney and colon specimens were obtained by laparotomy. The right kidney specimens were subjected to histological study. As well as the terminal 4 cm of the distal part of descending colon, approximately 2 cm above the anal verge exposure, was divided into 2 specimens: one for biochemical study and the other for histological study.

Biochemical Study

Specimens from the distal segment of descending colon were homogenized and analyzed to assess:

Malondialdehyde (MDA): using Elabscience® MDA assay colorimetry kit (Catalogue no. E-BC-K025-S, Texas, USA) to determine lipid peroxidation in colon[22].

Enzyme linked immunosorbent assay (ELISA) for TNF-α: using Cusabio® rat TNF-α ELISA protocol (Catalog no.CSB-E11987r, Houston, USA). TNF-α is a marker for inflammation[23].

Polymerase chain reaction (PCR) for PPAR-γ RNA expression: using Promega® SV Total RNA Isolation System (catalogue no. Z3101, Madison, USA). Real-time qPCR amplification & assessment were done through an Applied Biosystem, software version 3.1 (StepOne™, USA). The qPCR assay of the primer sets for PPAR-γ were: F: 5′-AACCGGAACAA-ATGCCAGTA-3′R:5′ TGGCAGCAGTGGAAGAATCG-3′ and ß-Actin: F: 5′-CCCATCTATGAGGGTTACGC -3R: 5′-TTTAATGTCACGCACGATTTC -3'.

Faecal and blood samples as well as colonic samples for biochemical study were analyzed in Biochemistry Department, Faculty of Medicine, Cairo University.

Histological Study

Specimens from right kidney and colon were fixed in 10% formalin for twenty-four hours followed by processing for paraffin blocks; Serial sections 6μm thick were stained by the followings stains[24]:

Hematoxylin &Eosin (H&E), for kidney and colon histological structure examination.

Masson's trichrome stain, to assess collagen fiber deposition in kidney.

Alcian blue / Periodic acid Schiff (PAS) stain for illustration of mucin secreting cells in colon. Alcian blue for acidic mucin (stains blue) and PAS stain for neutral mucin (stains magenta). Neutral mucins are mainly present in the cranial portions of the digestive tract while acidic mucins are predominately located in the distal part of colon[25].

Immunohistochemical stain for claudin-1, a rabbit polyclonal antibody (E-AB-30939, Elabscience Texas, USA). Claudin-1 is a transmembrane protein of colonic epithelium tight junctions and is involved in the regulation of paracellular transport of molecules and in intracellular signaling[26]. It appeared as memberanous reaction.

Immunohistochemical stain for caspase-3, a rabbit polyclonal antibody E-AB-63510, Elabscience Texas, USA). It is used to detect cellular apoptosis in colonic tissue[27]. It appeared as cytoplasmic immunoreactivity.

Immunostaining was done using avidin-biotin technique[24] by:

1. Boiling of colonic sections for antigen retrieval in citrate buffer of 10 mM (Cat No. 005000) pH 6 for ten minutes.
2. Followed by cooling of sections for twenty minutes at room temperature.
3. Then incubation with primary antibodies for 60 minutes. Corresponding to manufacturer’s datasheet, the optimal dilution was 1:100-1:300 for claudin-1, and 1:50-1:200 for caspase-3 antibodies.
4. Staining was performed by Ultravision One Detection System (Cat No. TL - 060- HLJ) and Lab Vision Mayer's hematoxylin counterstaining (Cat No. TA- 060- MH).

The following were purchased from Labvision, ThermoFisher scientific, USA: Ultravision One Detection System, citrate buffer, in addition to Ultravision Mayer's hematoxylin.

Claudine-1 positive control showed brown membranous expression in liver. The positive control for caspase-3 illustrated as brown cytoplasmic reaction in heart. Whereas the negative control colonic sections were performed by the former steps without the step of the primary antibodies.

Morphometric Study

"Leica Qwin 500 C" image analyzer computer system Ltd. (Cambridge, England) was utilized to analyze measurements of the following parameters:

- The area percent of collagen in renal sections stained with Masson's Trichrome stain.
- The total number of Alcian blue/ PAS positive mucin secreting cells in alcian blue/ PAS-stained colonic sections per high power field.
- The percentage of PAS positive stained mucin secreting cells (neutral mucin) according to the following equation:

Neutral mucin secreting cells percentage = (Number of PAS positive cells)/(Total number of Acian blue/PAS positive cells) X 100

- The area percent of immuno-positive reaction in colonic sections stained for claudin-1 and caspase-3.

All parameters were measured in 10 non-overlapping randomly selected fields (x400) in 5 sections of 5 animals in all groups except for area percent of collagen which was assessed in 10 non-overlapping randomly chosen fields (x200) in 5 sections of 5 animals from all groups.

Histological as well as morphometric studies were accomplished at the Histology Department, Faculty of Medicine, Cairo University.

Statistical study

Quantitative values were detected as mean & standard deviation. Comparison was performed through applying one-way analysis-of-variance, followed by post-hoc tukey test[28] using SPSS software version 21. Probability values (P) <0.05 were significant.

RESULTS

General observations

- Regarding the mortality rate, no rats died during the experiment in all experimental groups.
- Subgroups IA, IB & IC showed the same biochemical and histological findings, so they were identified as group I.

Biochemical and statistical results

Serum creatinine level: (Figure 1a)

In comparison to group I, a significant rise in serum creatinine value in groups II, III&IV was illustrated. However, group V demonstrated a non-significant increase. A non-significant reduction in creatinine level was illustrated in group III relative to group II. In addition, a non-significant decrease was noticed in group V compared to group IV. There was a significantly lower value in groups IV and V relative to group III.

Colonic MDA and TNF-α levels: (Figure 1b)

A rise in MDA and TNF-α appeared significant in all groups versus control group. A non-significant lower value of MDA & TNF-α was recoded in recovery group relative to CKD model group. There was a significant diminution in MDA and TNF-α level in groups IV and V versus group III. Additionally, a significant diminution in group V versus IV was demonstrated.

Colonic PPAR- γ expression: (Figure 1c)

Reduced PPAR -γ expression was statistically significant in all groups versus control group except in group V where a non-significant reduction was detected. Moreover, a non-significant increase in PPAR-γ expression in group III versus group II was noticed. Compared to group III, groups IV and V recorded a significant rise in PPAR-γ expression. Additionally, a non-significant rise in group PIO-CS NPs (group V) versus CS NPs (group IV) was demonstrated.

Faecal lactobacilli expression: (Figure 1c)

A significant reduction in faecal lactobacilli expression in whole groups relative to group I was illustrated, but in group V a non-significant diminution was detected. Group III showed a non-significant rise in stool lactobacilli expression versus group II. Compared to group III, group V recorded a significant rise while group IV showed a non-significant elevation. Additionally, there was a non-significant rise in group V relative to group IV.

Histological results

H&E-stained sections of the kidney

Control group (Figure 2a): Histologically, cortical parenchyma with preserved architecture of Malpighian renal corpuscles and normal renal tubules was illustrated. Renal corpuscles showed regular Bowman's spaces around glomeruli. Kidney tubules exhibited deeply acidophilic cytoplasm, vesicular nuclei, as well as preserved brush borders in proximal convoluted tubules.

CKD model group (Figure 2b) and Recovery group (Figure 2c): Examination of H&E-stained kidney sections illustrated disrupted renal cortical architecture. Malpighian renal corpuscles appeared with widened Bowman's spaces and shrunken glomeruli. Kidney tubules showed pyknotic nuclei, loss of brush borders and widened lumina. Infiltration of renal interstitium with inflammatory cells was noticed.

CS NPs group (Figure 2d): H&E-stained renal sections revealed Malpighian renal corpuscles with widened Bowman's spaces surrounding the glomeruli. In addition, pyknotic nuclei and interrupted brush borders were observed in some renal tubules.

PIO-CS NPs group (Figure 2e): Administration of PIO-CS NPs revealed apparently normal cortical parenchyma with preserved architecture of Malpighian renal corpuscles and renal tubules. The Renal corpuscles

consisted of glomeruli & Bowman's spaces. Renal tubules exhibited an apparently normal structure with vesicular nuclei. Proximal convoluted tubules with preserved apical brush borders were noticed.

Masson's trichrome stained renal sections

Group I section's demonstrated minimal collagen fibers around Malpighian renal corpuscle as well as renal tubules (Figure 3a). In CKD model group more collagen fibers appeared around Malpighian renal corpuscles as well as around renal tubules (Figure 3b). Also, the recovery group revealed an apparently increased collagen fibers deposition (Figure 3c) compared to the control group. With CS NPs treatment some collagen fibers deposition was noticed (Figure 3d). Following PIO-CS NPs administration there was few collagen fibers deposition around renal corpuscles and renal tubules (Figure 3e).

H&E-stained sections of the colonic mucosa

Control group (Figure 4a): Examination of control rat colon sections showed intact surface simple columnar epithelium and well-organized intestinal crypts separated with loose connective tissue containing few inflammatory cells. The surface and crypts were lined by tall columnar cells that demonstrated apical brush borders and basally located oval vesicular nuclei. Many goblet cells with basal nuclei and cytoplasmic vacuolation were observed along the lining of surface and crypts.

CKD model group (Figure 4b) and Recovery group (Figure 4c): Microscopically it showed loss of surface epithelium with distortion of intestinal crypt structure. Most epithelial cells exhibited darkly stained nuclei. Goblet cells appeared few in the lining epithelium of the crypts. Marked inflammatory infiltration was clearly observed in connective tissue and infiltrating the crypts.

CS NPs group (Figure 4d): The H&E-stained colonic sections showed few areas of disrupted surface epithelium. Some crypts were distorted and exhibited absorptive cells with deeply stained nuclei and some goblet cells. Additionally, some inflammatory cells were seen in the underlying connective tissue and infiltrating the intestinal crypts.

PIO-CS NPs group (Figure 4e): Colon sections of rats treated with PIO-CS NPs illustrated apparently intact colonic mucosa with intact surface simple columnar epithelium and well-organized intestinal crypts. Some goblet cells were observed along the lining of the surface and the crypts. Minimal inflammatory cellular infiltration was illustrated.

Alcian blue/PAS-stained colonic sections

The control rat's colon sections revealed widely distributed mucin secreting cells with alcian blue/PAS positive staining lining the surface and intestinal crypts (Figure 5a). However, in the CKD model and recovery groups few goblet cells with positive reaction for alcian blue/PAS was detected (Figures 5 b,c). As regards the CS NPs group, many mucin secreting cells exhibited Alcian blue/PAS positive reaction (Figure 5d). While PIO-CS NPs showed Alcian blue/PAS positive reaction in numerous goblet cells (Figure 5e).

Claudin-1 immuno-stained sections of the colon

The negative control colonic sections (Figure 6a) showed negative immunostaining after skipping the step of claudin-1 primary antibody.

The control group illustrated numerous positive membranous reactions in epithelial cells lining the surface and crypts. Few cells with positive cytoplasmic reaction were seen in the lamina propria (Figure 6b). In CKD model and recovery rat's sections, membranous immunoreaction was detected in a few epithelial cells. Also, a few cells with positive cytoplasmic reaction were observed in the connective tissue between crypts (Figures 6 c,d). Sections of the colon of CS NPs treated rats illustrated many epithelial cells with positive membranous reaction and few connective tissue cells with positive cytoplasmic reaction (Figure 6e). In PIO-CS NPs sections, positive membranous reaction was noticed in multiple epithelial cells, as well as there were few cells in the lamina propria with positive cytoplasmic reaction (Figure 6f).

Caspase-3 immune-stained sections of the colon

The negative control sections of colon (Figure 7a) demonstrating negative immunostaining with exclusion of adding the caspase-3 primary antibody.

In the control group positive cytoplasmic immunoreactivity in a few epithelial cells and connective tissue cells were detected (Figure 7b). In CKD and recovery groups, colon sections showed abundant positive cytoplasmic and /or nuclear reaction in the epithelial cells as well as connective tissue cells (Figures 7 c,d). On the other hand, CS NPs sections demonstrated positive reactivity in the cytoplasm of multiple epithelial and connective tissue cells (Figure 7e). In PIO-CS NPs, some cells with positive cytoplasmic immunostaining were demonstrated in the epithelium and lamina propria (Figure 7f).

Morphometric and statistical results

Mean area percent of collagen in the Masson's trichrome-stained renal sections: (Figure 3f)

Relative to control group, an elevation was significant in whole groups except group V where there was a non-significant rise. Additionally, a non-significant rise in recovery group versus model group was shown. The reduction of mean area percent appeared significant in group V and non-significant in group IV in comparison to recovery group. As regards group V, the decrease in the mean area percent of collagen relative to group IV was significant.

Mean total number of Alcian blue/ PAS positive mucin secreting cells in colonic sections: (Figure 5f)

A diminution in the mean total number of mucin secreting cells in all groups versus control group was statistically significant. Additionally, a non-significant rise was demonstrated in the recovery group versus CKD model group. However, a significant rise in groups IV & V versus group III was detected. Group V exhibited an elevation which was significant relative to group IV.

The mean percentage of PAS positive cells to the total Alcian blue/ PAS positive cells in colonic sections: (Figure 5g)

The percentage of PAS positive cells (neutral mucin) was significantly raised in all groups except in group V where a non-significant elevation was illustrated versus control group. Additionally, a non-significant reduction was noticed in the recovery group versus model group. While a reduction in percentage of neutral mucin secreting cells in groups CS NPs and PIO-CS NPs versus recovery group was significant. Group V illustrated a diminution that was significant versus group IV.

Mean area percent of claudin-1 positive immunoreaction in colonic sections: (Figure 6g)

Diminution in mean area percent of claudin-1 positive immunoreactivity in all groups versus control group was significant, but in groups IV and V a non-significant decrease was shown. Additionally, a non-significant rise was noted in recovery group relative to CKD model group. In comparison to group III, an elevation was significantly detected in groups CS NPs & PIO-CS NPS. Group V illustrated a non-significant rise versus group IV.

Mean area percent of caspase-3 positive immunoreaction in colonic sections: (Figure 7g)

As regards group I, a significant elevation in all groups was recorded. Moreover, a non-significant reduction was noticed in the recovery group versus the model group. Relative to group III, a reduction was shown in groups IV and V that appeared significant. Group V illustrated a significant diminution versus group IV.

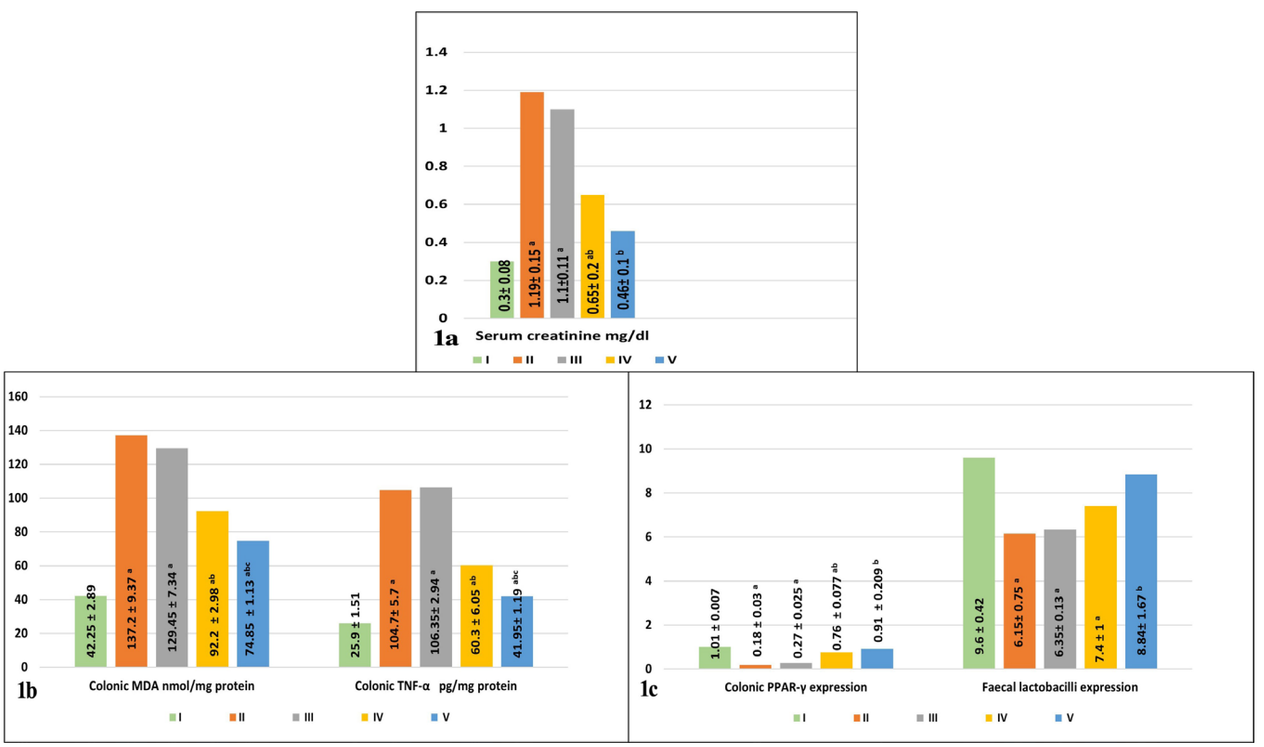

Fig. 1: Showing mean values of:
1a: Serum creatinine level.
1b: Colonic MDA and TNF-α levels.
1c: Colonic PPAR- γ and faecal lactobacilli expression.
[a in comparison to control group, b in comparison to group III, & c in comparison to group IV (significant difference at $P < 0.05$)]

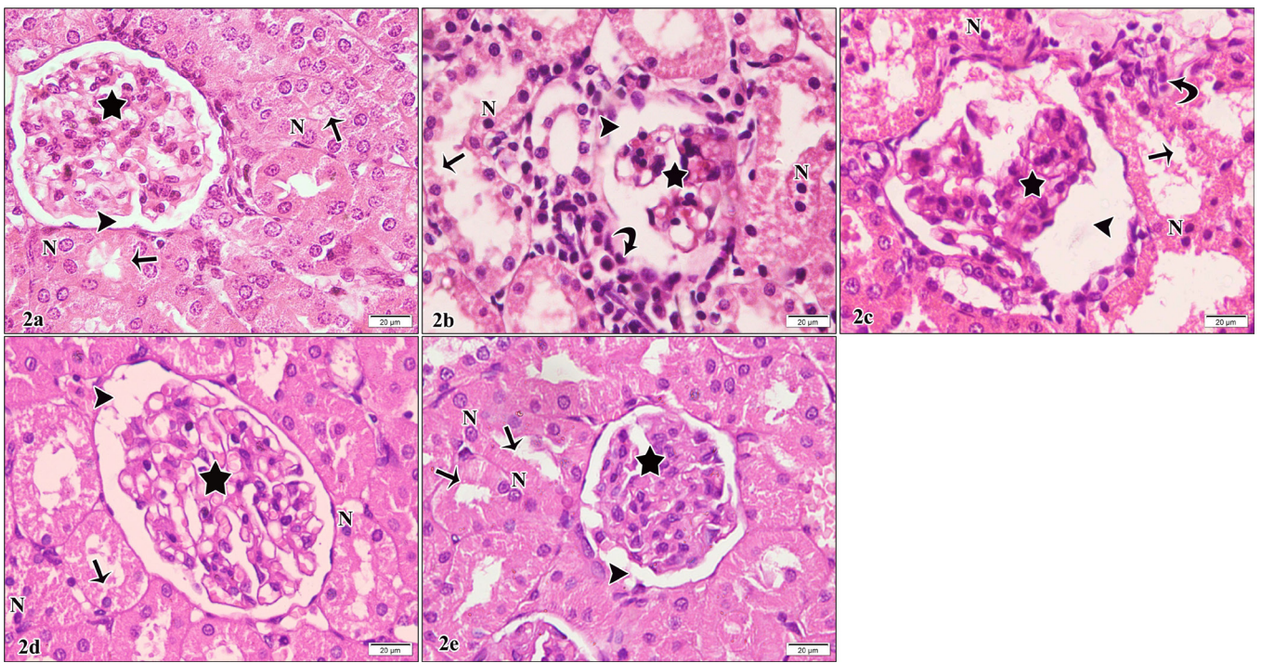

Fig. 2: Photomicrographs of H&E-stained kidney sections of: **2a** (Control group): Illustrating normal structure of renal cortex, renal corpuscle consists of glomerulus (star) & is surrounded by regular Bowman's space (arrowhead). Proximal convoluted kidney tubules exhibit preserved brush borders (straight arrows), deeply acidophilic cytoplasm and vesicular nuclei (N). **2b** (CKD model group) and **2c** (Recovery group): Showing disrupted architecture of Malpighian corpuscle with shrunken glomerulus (star) surrounded by widened capsular space (arrowhead). Renal tubules with widened lumina and disrupted brush border (straight arrow) are noticed. Besides, epithelial tubular cells show pyknotic nuclei (N). Inflammatory infiltration is seen around renal corpuscle (curved arrow). **2d** (CS NPs group): Showing renal corpuscle with widened Bowman's space (arrowhead) surrounding glomerulus (star). Some tubular epithelial cells have darkly stained nuclei (N) and disrupted brush border (straight arrow). **2e** (PIO-CS NPs group): Illustrating normal structure of Malpighian corpuscle formed of glomerulus (star) surrounded by urinary space (arrowhead). Apparently normal proximal convoluted tubules with vesicular nuclei (N) and preserved brush borders (straight arrows) are noticed. (H&E, x 400)

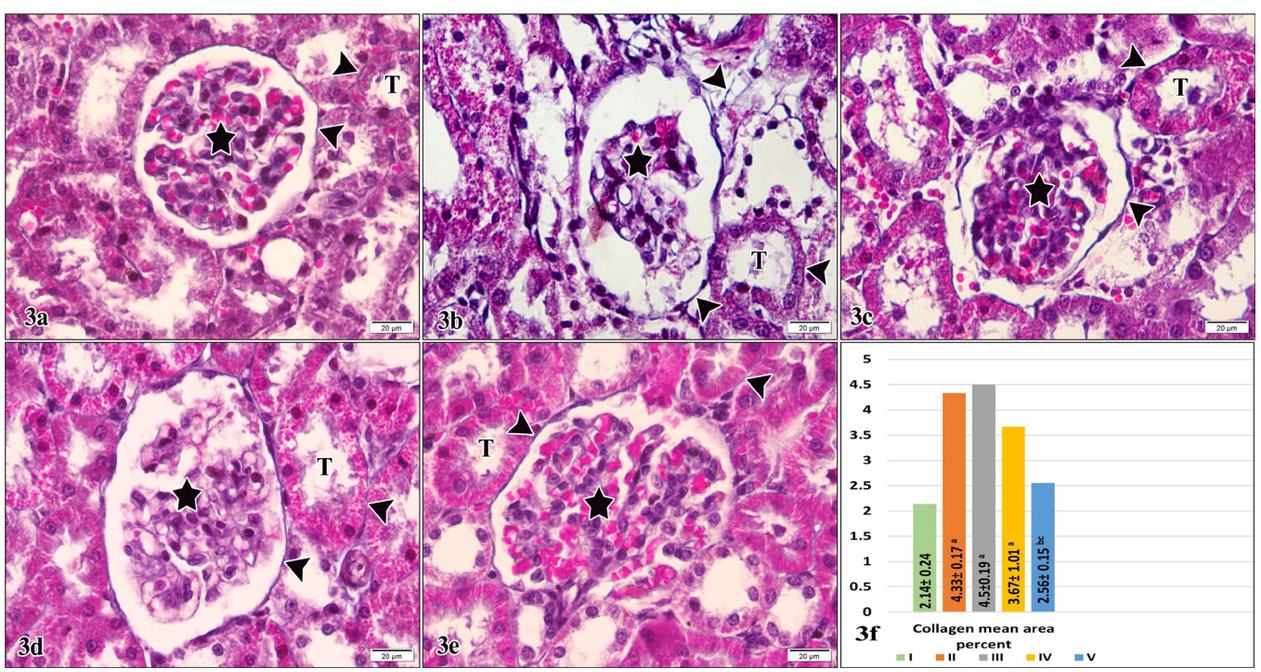

Fig. 3: Photomicrographs of Masson's trichrome-stained kidney sections of: **3a** (Control group): Demonstrating minimal collagen fibers (arrowheads) around Malpighian renal corpuscle (star) and kidney tubules (T). **3b** (CKD model group): Illustrating more collagen fibers deposition (arrowheads) around Malpighian renal corpuscle (star) and tubules (T). **3c** (Recovery group): Showing apparently increased collagen fibers deposition (arrowheads) around renal corpuscle (star) and renal tubules (T). **3d** (CS NPs group): Demonstrating some collagen fibers deposition (arrowheads) around Malpighian corpuscle (star) and in between tubules (T). **3e** (PIO-CS NPs group): Showing few collagen fibers (arrowheads) around Malpighian renal corpuscle (star) and in between tubules (T). (Masson's trichrome, x 400). **3f:** Demonstrating the mean area percentage of collagen fibers. [a in comparison to control group, b in comparison to group III, & c in comparison to group IV (significant difference at $P < 0.05$)]

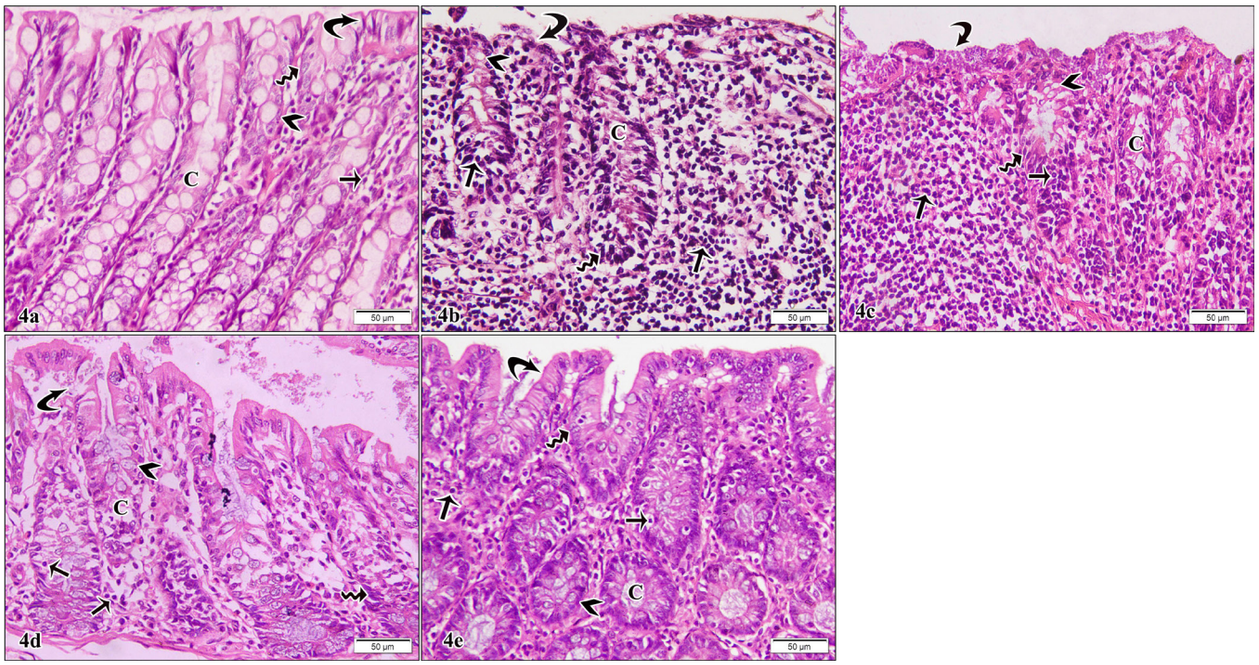

Fig. 4: Photomicrographs of H&E-stained colon sections of: **4a** (Control group): Exhibiting intact surface simple columnar epithelium (curved arrow) and well-arranged intestinal crypts (C) separated with loose connective tissue containing few inflammatory cells (straight arrow). Columnar epithelial cells (wavy arrow) have basal oval vesicular nuclei, and apical brush borders. Goblet cells (arrowhead) show cytoplasmic vacuolation and basal nuclei. **4b** (CKD model group) and **4c** (Recovery group): Illustrating lost surface epithelium (curved arrow). Crypts (C) with distorted architecture are lined with epithelial cells with deeply stained nuclei (wavy arrow) and apparently few goblet cells (arrowhead). Obvious inflammatory cells (straight arrows) infiltrating the underlying connective tissue and crypts are noticed. **4d** (CS NPs group): Showing localized area of disrupted surface simple columnar epithelium (curved arrow). Distorted intestinal crypts (C) with apparently some goblet cells are observed (arrowhead). Also, some absorptive cells exhibited pyknotic nuclei (wavy arrow). Minimal inflammatory infiltration (straight arrows) is noticed in the underlying connective tissue and within colonic crypts. **4e** PIO-CS NPs group: Demonstrating intact surface simple columnar epithelium (curved arrow) and normally arranged crypts (C). Apparently normal columnar absorptive cells (wavy arrow) and some goblet cells (arrowhead) are noticed lining the surface and the colonic crypts. Minimal inflammatory infiltration (straight arrows) is observed in colonic crypts and in the lamina propria. (H&E, x 200)

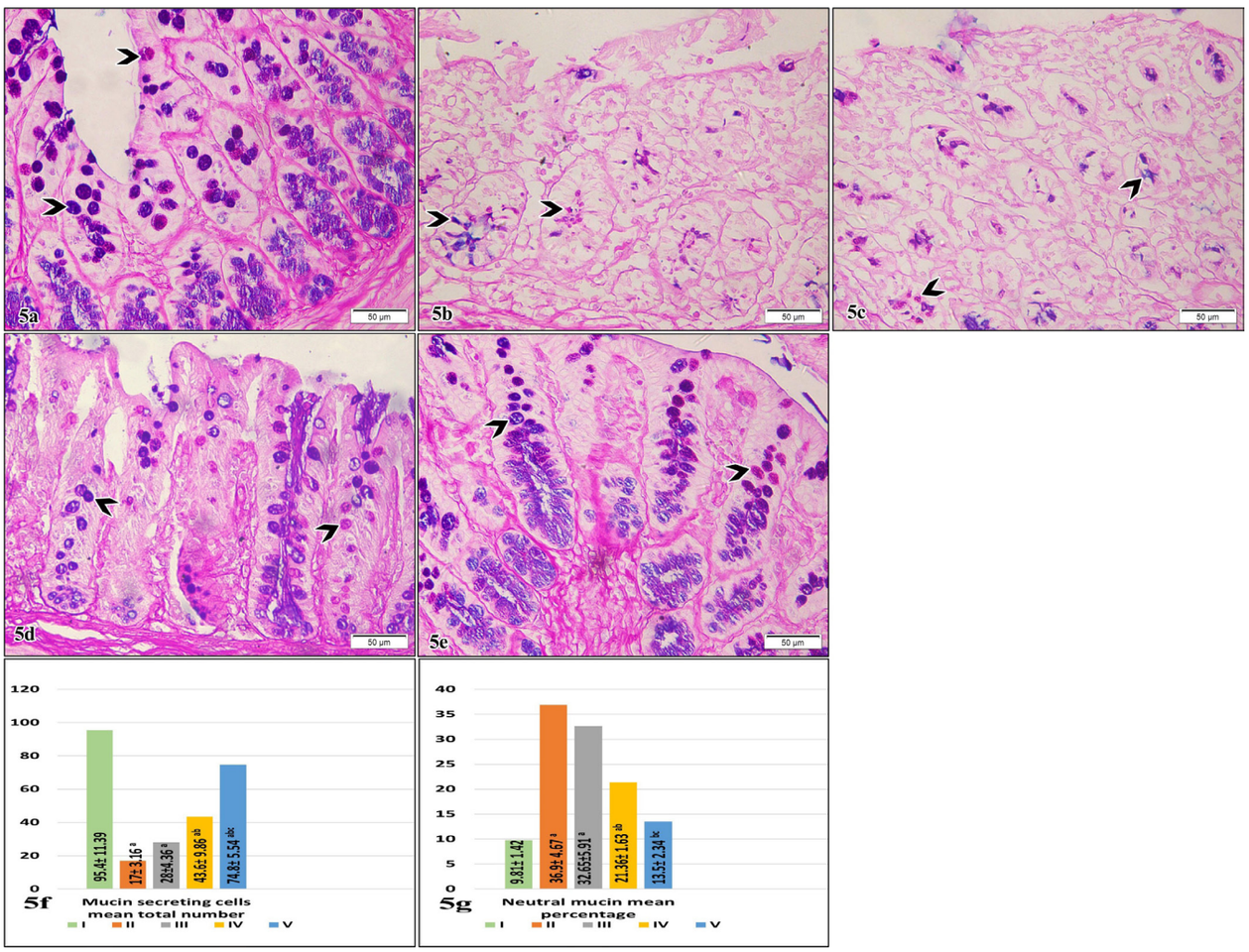

Fig. 5: Photomicrographs of Alcian blue /PAS-stained colon sections of: **5a** (Control group): Showing widely distributed goblet cells with positive alcian blue/ PAS reaction (arrowheads) lining the surface and the intestinal crypts of the colon. **5b** (CKD model group) and **5c** (Recovery group): Showing alcian blue/ PAS reaction (arrowheads) in few goblet cells lining the colonic crypts. **5d** (CS NPs group): Illustrating positive alcian blue/PAS reaction (arrowheads) in many goblet cells lining the surface and crypts of the colon. **5e** (PIO-CS NPs group): Showing numerous goblet cells with positive alcian blue /PAS reaction (arrowheads) lining the intestinal crypts. (Alcian blue/PAS, x 200)
5f: Demonstrating the mean total number of Alcian blue/PAS positive mucin secreting cells. **5g:** Demonstrating the mean percentage of PAS positive mucin secreting cells. [a in comparison to control group, b in comparison to group III, & c in comparison to group IV (significant difference at $P < 0.05$)]

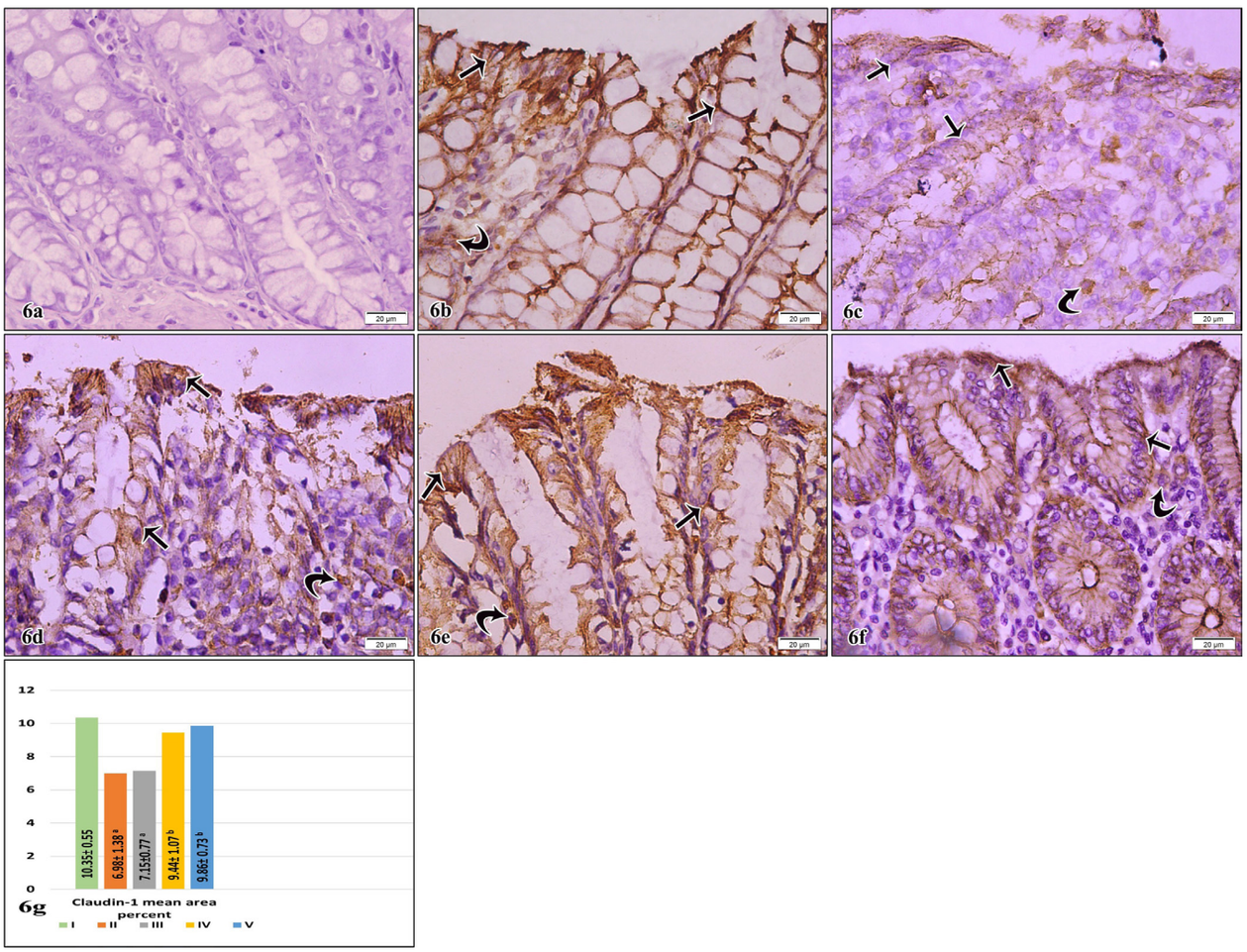

Fig. 6: Photomicrographs of claudin-1 immuno-stained colon sections of: **6a** (Negative control section of colon): illustrating negative immunoreaction. (x 400) **6b** (Control group): Illustrating positive membranous immunostaining in many epithelial cells lining the surface and crypts of the colon (straight arrows). Few connective tissue cells with positive cytoplasmic reaction are seen (curved arrow). **6c** (CKD model group) and **6d** (Recovery group): Demonstrating scanty positive membranous reaction in the epithelial cells of the surface and crypts (straight arrows). Few cells with positive cytoplasmic reaction are also detected in the connective tissue (curved arrow). **6e** (CS NPs group): Showing positive membranous reactivity in many epithelial cells lining surface and crypts (straight arrows). Also, positive cytoplasmic reactions are noticed in a few cells in lamina propria (curved arrow). **6f** (PIO-CS NPs group): Illustrating positive membranous reaction in multiple cells lining the surface and the crypts (straight arrows). Few cells with positive cytoplasmic reaction are noticed in the connective tissue (curved arrow). (Claudin-1, x 400)
6g: Demonstrating the mean area percentage of claudin-1 positive reaction. [a in comparison to control group & b in comparison to group III (significant difference at $P < 0.05$)]

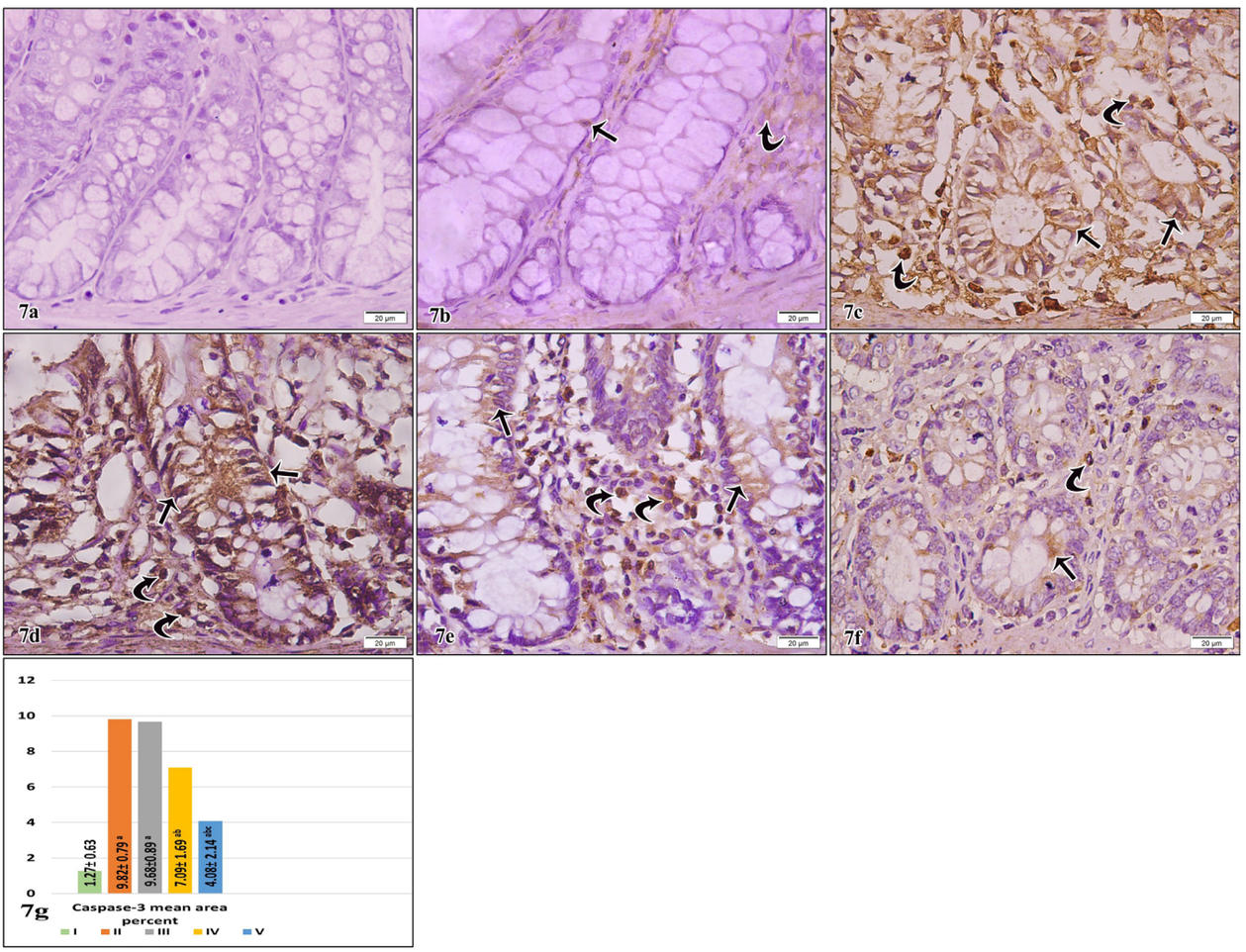

Fig. 7: Photomicrographs of caspase-3 immunostained colon sections of: **7a** (Negative control section of colonic tissue): showing negative immunostaining. (x 400) **7b** (Control group): Illustrating positive cytoplasmic reaction in few epithelial cells (straight arrow) and connective tissue cells (curved arrow). **7c** (CKD model group) and **7d** (Recovery group): Showing abundant positive cytoplasmic and /or nuclear reaction within the epithelial cells (straight arrows) and the underlying connective tissue cells (curved arrows). **7e** (CS NPs group): Showing positive cytoplasmic reactivity in multiple epithelial cells lining the crypts (straight arrows) and in cytoplasm and /or nuclei of connective tissue cells (curved arrows). **7f** (PIO-CS NPs group): Illustrating positive cytoplasmic reaction in some colonic epithelial cells (straight arrow) and few cells within the surrounding connective tissue (curved arrow). (Caspase-3, x 400) **7g:** Demonstrating the mean area percentage of caspase-3 positive reaction. [a in comparison to control group, b in comparison to group III, & c in comparison to group IV (significant difference at $P < 0.05$)]

DISCUSSION

The present work was accomplished to present a model of adenine induced CKD associated colitis and to clarify the link between kidney and gut microbiota (the kidney-gut axis). As well as to evaluate the therapeutic impact of chitosan nanoparticles (CS NPs) versus pioglitazone loaded chitosan nanoparticles (PIO-CS NPs).

In the current study, adenine was administered for three weeks to induce CKD. Assessment of serum creatinine levels showed significant elevation in CKD model group relative to control group. This result was similar to another study featuring adenine induced CKD in a rat model where increased serum levels of creatinine, urea, magnesium and phosphorus were observed. These changes indicate deterioration of kidney function in a rat model[29].

The CKD model group H&E-stained renal sections showed Malpighian corpuscles with shrunken glomeruli and widened Bowman's spaces. Renal tubules showed signs of epithelial degeneration as pyknotic nuclei and loss of brush borders. Similar observations were noticed by de Frutos *et al*.,[30]. Additionally, a significant increase in collagen fibers deposition was demonstrated versus group I. This agrees with former researchers who attributed the increased mRNA expression of collagen I and fibronectin to upregulation of transforming growth factor-β (TGF-β) which has a main role in renal fibrosis induction[31]. The collagen deposition is a dynamic process including inflammatory infiltration, fibroblast proliferation and stimulation, and microvascular degeneration[32]. Several investigators explained the previous findings by the intake of adenine in doses greater than the body's metabolic need which is considered harmful. Crystallization of its metabolite 2,8 dihydroxy adenine and precipitation in the kidney tubules is the main pathological outline for progression of CKD in animal models. First, tubular

dilatation followed by tubular degeneration, then interstitial fibrosis follows. These structural abnormalities are accompanied by functional disturbance of the renal parameters as well as progression of CKD associated complications[33].

Analysis of faecal lactobacilli expression (a beneficial gut microbe) in CKD group illustrated a significant reduction in comparison to group I. Such imbalance was similarly observed in mice of CKD model induced by adenine[34].

As CKD progresses, uremic toxins start to build up in the tissues due to the inability of the kidney to excrete toxic metabolites. The increased blood urea diffuses into the intestinal lumen where it is metabolized by urase of bacteria into ammonia and ammonium hydroxide which has a damaging effect on intestinal mucosa[35]. This was similarly demonstrated in a former work where intestinal dysbiosis was a consequence of CKD induction in a rat model. Intestinal dysbiosis results in decreased faecal content of short chain fatty acids (beneficial substrates of nutrient fermentation by intestinal microbes) and increased serum levels of uremic toxins[36].

Measurement of colonic MDA (oxidative stress marker) and TNF-α (inflammatory marker) in CKD model group showed a significant rise versus group I. This could be explained by dysbiosis which is usually associated with inflammation and oxidative stress resulted from dysfunction of intestinal barrier and elevated intestinal permeability, causing endotoxin and uremic toxins translocation to the blood[37,38]. Gut microbiota endotoxin stimulates inflammatory cells with the release of proinflammatory cytokines[39]. As well as uremic toxins, indoxyl sulfate and p-cresol, stimulate the production of ROS, aggravating the oxidative stress state allowing progression of CKD creating a vicious circle[40].

The recorded colonic inflammatory state in CKD group matched the significant decrease of PPAR-γ expression in the colonic tissue versus group I. This result is in line with the findings of prior research where it recorded decreased PPAR-γ in colitis model[41]. PPAR-γ promotes anti-inflammatory signaling pathway and acts as a regulator for regulatory T (Treg) as well as T helper 17 (Th17) cells differentiation[42]. It enhances Treg differentiation and represses the Th17 cells differentiation[43]. Additionally, PPAR-γ ligands can block the activation of macrophages and inflammatory factors secretion like TNF-α, IL-6, and Il-1β. Therefore, the repressed anti-inflammatory response stimulated by reduction of colonic PPAR-γ might aggravate the inflammatory condition[44].

Microscopically, colonic H&E-stained sections of CKD model group showed distorted crypt architecture, shedding of surface epithelium, in addition to the presence of pyknotic nuclei in multiple colonic cells and diffuse inflammatory infiltrate of the crypts and underlying connective tissue. Matching results were found in a mouse model of induced dysbiosis[34,45]. These findings were attributed to the cross talk between intestinal epithelium and gut microbiota. Intestinal microbiota imbalance leads to inflammatory pathway activation, metabolism of toxins inside intestinal lumen and destruction of tight junction associated proteins.

The noticed inflammatory cells infiltrating the crypt in CKD model group indicated active colonic inflammation and was described formerly as cryptitis or crypt abscess[46]. Similar results were demonstrated in a mouse model of colonic dysbiosis along with destruction of mucosal architecture, increased intestinal permeability and increased inflammatory markers as TNF-α and IL-1β[47].

With alcian blue/PAS stain, sections of the colon in CKD model rats exhibited a significant low value of the mean total number of alcian blue/PAS positive mucin secreting cells versus group I. Similar results were observed in a mouse model of adenine induced CKD[48]. This could be explained by dysbiosis resulting in damage of gut epithelium, as microbiota does not contribute to production of short chain fatty acid, thus suppress upregulation of hypoxia inducible factor-1 (HIF), a factor necessary for transcription of mucin proteins that protect the gut barrier integrity[49]. Interestingly, it has been recently demonstrated that mucin is considered as prime in the maintenance of a "healthy" microbiota, protecting them from chemical-induced colitis[50].

Additionally, a significant rise in percentage of PAS positive mucin secreting cells was recorded. This finding is concomitant with experimentally induced mucosal barrier injury[51] and dextran sodium sulfate colitis model[52] where they recorded decreased percentage of acidic mucin and increased percentage of neutral mucin indicating a shift to neutral mucin. This could be explained by alterations in microbiota and consequently affect mucin composition. Colonization and proliferation of microbiota widely affect composition of mucin, by the production of mucin-specific glycosidases, glycosulfatases as well as proteases[53].

The intestinal barrier is maintained by interactions between diversity of factors, including mucous gel layer, secretory IgA, and intercellular tight junctions[54]. Immunohistochemically in the present work, a significant low values of mean area percentage of claudin-1 in colonic sections was noticed in the CKD model rats in relation to control rat's sections. This could be linked to protein-bound uremic toxins, particularly their free forms, stack in the intestinal mucosa and can mediate toxic impacts on intestinal barrier integrity and in turn, impair tight junctions' structure[55]. This finding is in concordance with surgical nephrectomy model of CKD, where there was decreased multiple tight junction expression as zona occludens 1, occludin, claudin-1 and claudin-2. Also, it showed indistinct tight junctions and widening of intercellular space of the colonic epithelium by electron microscope[56].

Additionally in the present work, a positive cytoplasmic reaction of claudin-1 was noticed in a few cells in the

connective tissue lamina propria. Cytoplasmic localization of claudin-1 has been thought to be due to involvement of claudin-1 in cellular functions such as regulation of gene transcription, cellular proliferation, survival and signaling[57]. It was hypothesized that deficient epithelial barrier stimulates expression of claudin-1 in mononuclear inflammatory cells in lamina propria[58]. Expression has been demonstrated to be induced by TGF-β secreted by epithelial cells[59]. It was theorized that these cells are immune-modulatory macrophages that are activated to aid in resolution of the inflammatory response and repairing the damaged epithelial barrier[60].

Caspase-3 (an apoptotic marker) mean area percentage was significantly increased in CKD model group versus group I. Caspase-3 is an endo-protease enzyme that plays a key role in apoptosis. It is originally produced in an immature form; procaspase which is activated on need by proteolysis. Activation of caspase-3 is executed through two pathways; extrinsic and intrinsic. Extrinsic pathway is upregulated through surface receptors as TNF-α, while intrinsic pathway is activated through intracellular signals such as leakage of cytochrome C from mitochondria into cytoplasm[27] following an oxidative stress state and increased MDA level[61].

As regards recovery group, there was a minimal and insignificant improvement of all biochemical, histological, and morphometric results. This could be explained by self-recovery of renal tissue after cessation of injurious agent. As regards the mean area percentage of collagen, it exhibited a non-significant rise versus CKD model group. The insignificant difference of recovery group from CKD model group was similarly observed formerly as regards serum creatinine level, while there were increased uremic toxins and renal fibrosis 4 weeks following cessation of adenine intake[62]. In another study, no reversal of renal function to normal state occurred even after recovery periods of 8 weeks following induction of disease by adenine[63]. The controversy of the previously stated findings might be attributed to different models of adenine induced CKD using variable doses and durations.

In the present research, CS NPs were prepared through ionic gelation. Ionic gelation, the most commonly used technique, depends on the cross linking of positively charged chitosan groups to a polyanion. This method is preferred due to its quick preparation and low toxicity[64]. One of the key parameters during preparation of chitosan nanoparticles is degree of deacetylation (DD). This parameter determines the amount of available amino groups after extraction of acetyl group from the chitin structure. In the current study, chitosan nanoparticles with DD of 85% were used. This percentage is thought to have a smaller particle size and a perfect dispersity distribution[16].

Chitosan, a polysaccharide of natural sources, has attracted great interest in various medical applications because of its physical as well as chemical characteristics. Furthermore, it is used as a drug delivery method as being biodegradable, safe, and biocompatible[65]. In addition to controlling drug release, increasing their solubility and stability, and reducing their toxicity[66]. Aside from its role in drug delivery, chitosan has been thought to have anti-bacterial, anti-fungal and immune-modulatory effects[9].

Chitosan NPs administration following CKD induction detected a significant low value in serum creatinine versus recovery group. As well as H&E-stained renal sections showed some shrunken glomeruli with widened Bowman's spaces and some degenerated renal tubules while others appeared normal. These findings are concordant with former investigators who examined chitosan NPs treatment for carbon tetrachloride-induced nephrotoxicity[67]. The authors reported decreased levels of serum urea and creatinine, MDA, TNF-α and IL-1β in renal tissues along with marked amelioration of renal histopathological lesions and caspase-3 expression. The investigators linked these findings to the antioxidant, anti-inflammatory as well as anti-apoptotic effect of CS NPs. Also, they documented reduction of the expression of NF-κB, a major cellular mediator that prompts various pro-inflammatory cytokines, which is usually activated during oxidative stress.

Masson's trichrome stained renal sections of CS NPs administered animals illustrated a non-significant diminution in the mean area percent of collagen relative to recovery group. Similar observation was recorded following 5 weeks of CS NPs treatment in adenine model of chronic renal failure[68]. This was attributed to the anti-fibrotic influence of CS NPs that was mediated through suppression of expression of pro-fibrotic cytokines as tissue inhibitor of matrix metalloproteinase 1 & plasminogen activator 1 as well as collagen 1 expression in addition to enhancement of matrix metalloproteinase-1 expression.

In the current study in CS NPs group, the stool lactobacilli gene expression showed a non-significant rise versus the recovery group. This is in accordance with chitosan administration in ulcerative colitis model where chitosan adjusted the composition and diversity of intestinal flora by increase in beneficial bacterial species proliferation and decrease in pathogenic strains[69]. It was hypothesized that chitosan could act as a prebiotic through its N-acetylglucosamine fractions. It promotes proliferation and adhesion of beneficial intestinal flora in addition to prevention of binding of pathogenic bacteria to host epithelium[70].

Additionally, CS NPs treated rats exhibited a significant low level of colonic MDA & TNF-α and high PPAR-γ expression versus the recovery group. Along with improvement of histological alterations of colon and significant rise in mean total number of alcian blue/PAS-stained mucin secreting cells and significant reduction in neutral mucin percentage versus group III. This is similarly reported in different colitis models, where chitosan had increased expression of PPAR-γ that in turn inhibited the pro-inflammatory NF-κB pathway & decreased release of TNF-α, IL 1 and IL 6[71]. In addition

to alleviation of oxidative stress by increasing superoxide dismutase antioxidant enzymes[69], ameliorating colonic mucosa affection[72]. As well as CS NPs treatment increased mucin 2, a major intestinal protein secreted by goblet cells, promoting improvement of intestinal barrier integrity and function[71]. Further support backed immunohistochemically by the significant elevation in the mean area percentage of claudin-1 immunoreactivity relative to recovery group. This finding agrees with a prior study which reported that chitosan increased expression of occludin, claudin-1 and zona occludens-1 in ulcerative colitis model. It was postulated that chitosan modulated the expression of tight junction proteins through down regulation of TNF-α activity (which disrupt tight junction and barrier integrity)[26].

Aside from CS NPs anti-inflammatory and anti-antioxidant impacts, additional emphasize of CS NPs ameliorating effect was enlightened by significantly lower value of the mean area percent of caspase-3 versus the recovery group. These observations are in agreement with Zhang *et al*.,[73] where they noted that chitosan decreased percentage of early and late-stage apoptotic cells through decreased expression of multiple apoptotic markers as caspase-3, caspase-8, as well as TNF receptor-associated death domain in lipopolysaccharide-induced inflammation in intestinal epithelial cell line.

Pioglitazone does not induce hypoglycemia when used in non-diabetic rats as reported formerly[74]. This was suggested as it specifically targets the insulin resistance which characterizes type 2 diabetes mellitus[10].

According to biopharmaceutical classification system (BCS), pioglitazone is categorized as a class II drug that are characterized by having low water solubility leading to decrease in the drug's half-life, delay in its onset of action and increase in its elimination rate[75]. This emphasizes the need to increase amount of drug per dosage and increase number of doses which raise incidence of complications and incompliance. Different techniques have been used to enhance bioavailability of this class of drugs to ensure sustained and prolonged therapy.

In this study, CS NPs were used to enhance bioavailability of pioglitazone. CS NPs as a drug carrier system characterized by biodegradability and lack of toxicity[76]. The CS particles with sub-micron size increases gastrointestinal absorption, being cationic the mucoadhesion is enhanced, and eventually promotes the therapeutic effect of several drugs[77].

Multiple criteria control properties in drug loaded nanoparticles such as loading capacity & encapsulation efficiency. In the current study, formulation of PIO-CS NPs recruited a loading capacity of over 11%. Loading capacity is the percentage of the mass of the nanoparticle that is occupied by the drug. It has been theorized that loading capacity more than 10% is considered high and is beneficial in decreasing amount of nanomaterial used for drug delivery. This aids in reducing possible side effects of nanomaterial and diminishing cost of manufacture[78].

Encapsulation efficiency is the ability of the nanocarrier to entrap the drug. In the present study, PIO-CS NPs encapsulation efficiency reached more than 88%. This high encapsulation efficiency facilitates release of drug in a controlled manner and ensures maximum therapeutic effects to the target site and protect drug from metabolic breakdown[79].

Analysis of creatinine serum level of Pio-CS NPs group exhibited a significant reduction versus recovery group & a non-significant decrease versus CS NPs group. In addition, PIO-CS NPs ameliorated renal tissue alterations as evidenced by the apparently normal renal architecture. These findings were similarly observed in gentamycin induced nephrotoxicity where pioglitazone treatment improved biochemical profile, serum creatinine, and urea levels as well as histological picture of the kidney. Also, it inhibited NF-κB signaling pathways and release of inflammation cytokines as IL-1, IL-6 & TNF-α. In addition to reduction of oxidative stress parameters as MDA and increased antioxidants as catalase and superoxide dismutase in renal tissue[80].

The treatment with PIO-CS NPs also exhibited anti-fibrotic effect as Masson's trichrome stained sections demonstrated a significant diminution in mean area percent of collagen in comparison to recovery & CS NPs group. This agrees with another research where pioglitazone decreased both serum and tissue levels of TGF-β. It also decreased expression of other profibrotic markers as tissue inhibitor of matrix metalloproteinase 1 & connective tissue growth factor as well as expression of collagen types I and III[81].

Moreover, PIO-CS NPs administration complemented intestinal microbiota as it significantly increased expression levels of lactobacilli in stool samples of PIO-CS NPs group versus recovery group and non-significantly increased versus CS NPs group. These results are similar with Li *et al*.,[82] who observed reduced expression of pathogenic bacteria, and simultaneously increased expression of beneficial strains of bacteria by pioglitazone which in turn increased intestinal content of useful short chain fatty acids as acetate, butyrate & propionate as well as reduced serum endotoxin level.

Biochemical assessment of MDA and TNF-α levels in colonic tissue homogenate of PIO-CS NPs group showed a significant decrease relative to recovery and CS NPs groups. As regards PPAR-γ expression a significant rise versus recovery group and non-significant rise versus CS NPs group were detected. This agreed with a study of colitis model where increased PPAR-γ expression as well as decreased matrix metalloproteinase 9 and TNF-α expression were reported in mice treated with pioglitazone. Furthermore, pioglitazone ameliorated such condition through PPAR-γ receptor stimulation and suppression of NF-κB cellular pathways[83]. Similarly, several investigators noticed that pioglitazone had both anti-inflammatory and antioxidant impacts. Its anti-inflammatory effect was

exhibited through reducing levels of TNF-α & IL 6 in the serum and its antioxidant effect was through decreasing serum MDA level and increased glutathione level[84].

Additionally, in PIO-CS NPs H&E-stained sections, the colonic mucosa was apparently normal with intact architecture. Additionally, a significant rise in total number of goblet cells stained with alcian blue/PAS and significant reduction in percentage of neutral mucin were recorded in relation to recovery and CS NPs groups. Likewise in a prior work of induced gut dysbiosis, the reduced mucin and the elevated blood endotoxin levels were reversed following pioglitazone administration[82]. As regards the fact that multiple microbiota are present in the colon, the increase of acidic mucins suggests that the mucous viscosity is increased for more protection of the surface epithelial layer[85].

The previously mentioned findings of PIO-CS NPs group enhanced the intestinal barrier integrity which was proved immunohistochemically by the significant rise in mean area percentage of claudin-1 immune reactivity versus recovery and a non-significant rise versus CS NPs treated rats. These results match the findings of previous research which recorded enhanced intestinal barrier through upregulation of PPAR-γ expression in addition to zonula occludens-1 & claudin-5 following pioglitazone administration in a rat model of induced colitis[86].

Along with the antioxidant, anti-inflammatory, amelioration of alterations in gut microbiota and intestinal barrier, PIO-CS NPs illustrated antiapoptotic effect in the current research. It displayed a significant reduction in mean area percentage of caspase-3 immune positive reactivity relative to recovery and CS NPs groups. Similarly in earlier study, pioglitazone had ameliorated nonalcoholic steatohepatitis in mice model through down regulation of apoptosis as well as suppression of pro-inflammatory mediator's release as TNF-α, IL-6, NF-κB[87].

CONCLUSION

Adenine model was a reliable model for induction of colitis secondary to chronic kidney disease. Chitosan nanoparticle exhibited a considerable improvement in renal and colonic structure and function. However, Pioglitazone loaded chitosan nanoparticles exerted more powerful effect via its anti-inflammatory, antioxidant, antiapoptotic and PPAR-γ agonist effects. Along with its ameliorating effect on alterations of mucin secreting cells, intestinal integrity & junction, as well as intestinal microbiota.

RECOMMENDATIONS

Pioglitazone loaded chitosan nanoparticles might be considered after further trials for management of colitis and intestinal dysbiosis associated CKD. Experimental studies with longer durations are required to evaluate the long-term therapeutic effects of pioglitazone loaded chitosan nanoparticles in CKD associated colitis. In addition, it is necessary to explore the potential systemic adverse effects of pioglitazone loaded chitosan nanoparticles.

CONFLICT OF INTERESTS

There are no conflicts of interest.

REFERENCES

1. Collaboration GBDCKD. Global, regional, and national burden of chronic kidney disease, 1990–2017: a systematic analysis for the Global Burden of Disease Study 2017. Lancet. 2020;395: 709–733. doi:10.1016/S0140-6736(20)30045-3.
2. Charles C, Ferris A: Chronic Kidney Disease. Prim Care - Clin Off Pract. 2020 47:585-595. doi:10.1016/j.pop.2020.08.001.
3. Biruete A, Shin A, Kistler BM, Moe SM: Feeling gutted in chronic kidney disease (CKD): Gastrointestinal disorders and therapies to improve gastrointestinal health in individuals CKD, including those undergoing dialysis. Semin Dial. 2021:1-16. doi:10.1111/sdi.13030
4. Mechta Nielsen T, Frojk Juhl M, Feldt-Rasmussen B, Thomsen T. Adherence to medication in patients with chronic kidney disease: a systematic review of qualitative research. Clin Kidney J. 2018;11: 513–527. doi:10.1093/ckj/sfx140
5. Rysz J, Franczyk B, Ławi J, Olszewski R, Ciałkowska-Rysz A, Gluba-Brzózka A: The Impact of CKD on Uremic Toxins and Gut Microbiota. Toxins (Basel). 2021; 13:1-23. doi: 10.3390/toxins13040252.
6. Yusuf A, Almotairy ARZ, Henidi H, Alshehri OY, Aldughaim MS. Nanoparticles as Drug Delivery Systems: A Review of the Implication of Nanoparticles' Physicochemical Properties on Responses in Biological Systems. Polymers (Basel). 2023;15:1596. doi: 10.3390/polym15071596
7. Jain S, Cherukupalli SK, Mahmood A, Srividya G, Krishna RV, Kumar DS, Gautam S. Emerging nanoparticulate systems: Preparation techniques and stimuli responsive release characteristics. J Appl Pharm Sci. 2019; 9:130-143. doi:10.7324/JAPS.2019.90817
8. Garg, U.; Chauhan, S.; Nagaich, U.; Jain, N. Current Advances in Chitosan Nanoparticles Based Drug Delivery and Targeting. Adv. Pharm. Bull. 2019; 9: 195–204. doi: 10.15171/apb.2019.023.
9. jhaveri J, Raichura Z, Khan T, Momin M, Omri A: Chitosan nanoparticles-insight into properties, functionalization and applications in drug delivery and theranostics. Molecules. 2021; 26:1-29. doi:10.3390/molecules26020272
10. Hurren KM, Dunham MW. Are thiazolidinediones a preferred drug treatment for type 2 diabetes? Expert Opin Pharmacother. 2021; 22:131-133. doi: 10.1080/14656566.2020.1853100.

11. Hurren KM, Dunham MW. Understanding the impact of commonly utilized, non-insulin, glucose-lowering drugs on body weight in patients with type 2 diabetes. Expert Opin Pharmacother. 2018;19:1087–1095. doi: 10.1080/14656566.2018.1494727

12. Lefebvre M, Paulweber B, Fajas L, Woods J, McCrary C, Colombel JF, Najib J, Fruchart JC, Datz C, Vidal H, Desreumaux P, Auwerx J. Peroxisome proliferator-activated receptor gamma is induced during differentiation of colon epithelium cells. J Endocrinol. 1999;162:331-40. doi: 10.1677/joe.0.1620331.

13. Da Silva, S., A.V. Keita, S. Mohlin, S. Pahlman, V. Theodorou, I. Pahlman, J.P. Mattson, and J.D. Soderholm. A novel topical PPAR gamma agonist induces PPAR gamma activity in ulcerative colitis mucosa and prevents and reverses inflammation in induced colitis models. Inflammatory Bowel Diseases.2018; 24: 792–805. doi: 10.1093/ibd/izx079.

14. Bouguen, G., A. Langlois, M. Djouina, J. Branche, D. Koriche, E. Dewaeles, A. Mongy, J. Auwerx, J.F. Colombel, P. Desreumaux, L. Dubuquoy, and B. Bertin. Intestinal steroidogenesis controls PPAR gamma expression in the colon and is impaired during ulcerative colitis. Gut 2015; 64: 901–910. doi: 10.1136/gutjnl-2014-307618

15. Melekoglu E, Cetinkaya MA, Kepekci-Tekkeli SE, Kul O, Samur G: Effects of prebiotic oligofructose-enriched inulin on gut-derived uremic toxins and disease progression in rats with adenine-induced chronic kidney disease. PLoS One. 2021; 16:1-15. doi:10.1371/journal.pone.0258145

16. Rodrigues FC, Devi NG, Koteshwara KB, Thakur G: Investigating the effect of chitosan's degree of deacetylation on size of the nanoparticle. IOP Conf Ser Mater Sci Eng. 2020; 872:1-6. doi:10.1088/1757-899X/872/1/012109

17. Hasanin, Mohamed T., Elfeky SA, Mohamed MB , Amin RM. "Production of Well-Dispersed Aqueous Cross-Linked Chitosan-Based Nanomaterials as Alternative Antimicrobial Approach." Journal of Inorganic and Organometallic Polymers and Materials 2018; 28:1502-1510. DOI: 10.1007/s10904-018-0855-2

18. Borkhataria C, Patel R: Formulation and Evaluation of Pioglitazone Hydrochloride Loaded Biodegradable Nanoparticles. Chemistry (Easton). 2012; 1:157-163. doi: 68129e20d37330c397686ca5aa0a65c6c687cc19.

19. Byrav P, Medhi B, Prakash A, Chakrabarti A, Vaiphei K, Khanduja K: Comparative evaluation of different doses of PPAR-g agonist alone and in combination with sulfasalazine in experimentally induced inflammatory bowel disease in rats. Pharmacol Reports. 2013; 65:951-959. doi: 10.1016/s1734-1140(13)71076-4

20. Joseph NM and Sharma PK: Cross-linked nanoparticles of cytarabine: encapsulation, storage and in-*vitro* release. AJPP. 2007, 1, 10-13. https://academicjournals.org/journal/AJPP/article-full-text pdf/BEC00A932677

21. Abd El-Galil TI, ElGhamrawy TA, ElSadik AO: The Effect of N. Acetylcysteine and Ginger on Acetic Acid Induced Colitis in Adult Male Albino Rat: Histological, Immunohistochemical and Morphometric Study. J Cytol Histol. 2015; 3:1-8. doi:10.4172/2157-7099.s3-021

22. Su LJ, Zhang JH, Gomez H, *et al*.: Reactive Oxygen Species-Induced Lipid Peroxidation in Apoptosis, Autophagy, and Ferroptosis. Oxid Med Cell Longev. 2019; 2019:1-13. doi:10.1155/2019/5080843

23. Jhundoo H, Siefen T, Liang A, *et al*.: Anti-inflammatory activity of chitosan and 5-amino salicylic acid combinations in experimental colitis. Pharmaceutics. 2020; 12:1-16. doi:10.3390/pharmaceutics12111038

24. Suvarna KS, Layton C, Bancroft JD: The hematoxylins & eosin, connective tissue, mesenchymal tissue with their stains and Immunohistochemical techniques. In: Bancroft's Theory& Practice of Histological Techniques. 8th ed., Elsevier. 2019; pp:126–138, 153-175, 337-394. eBook ISBN: 9780702068867.

25. Brasil VP, Siqueira RM, Campos FG, Yoshitani MM, Pereira GP, Mendonça RLDS, Kanno DT, Pereira JA, Martinez CAR. Mucin levels in glands of the colonic mucosa of rats with diversion colitis subjected to enemas containing sucralfate and n-acetylcysteine alone or in combination. Acta Cir Bras. 2023;38:e384023. doi: 10.1590/acb384023

26. Wang J, Zhang C, Guo C, Li X: Chitosan ameliorates DSS-induced ulcerative colitis mice by enhancing intestinal barrier function and improving microflora. Int J Mol Sci. 2019; 20:1-12. doi:10.3390/ijms20225751

27. Asadi M, Taghizadeh S, Kaviani E, *et al*.: Caspase-3: Structure, function, and biotechnological aspects. Biotechnol Appl Biochem. 2022; 69:1633-1645. doi:10.1002/bab.2233

28. Dalmaijer ES, Nord CL, Astle DE. Statistical power for cluster analysis. BMC Bioinformatics.2022;23: 205-233. doi: 10.1186/s12859-022-04675-1.

29. Gori P, Patel A, Solanki N, Shah U, Patel V, Patel S: Protective effects of lycopene against adenine-induced chronic renal failure in rats. Indian J Physiol Pharmacol. 2021; 65:74-85. doi:10.25259/IJPP_188_2020

30. Chen R, Xu L, Zhang X, Sun G, Zeng W, Sun X: Protective effect and mechanism of Shenkang injection on adenine-induced chronic renal failure in rats. Acta Cir Bras. 2022; 37:1-10 doi:10.1590/acb370304

31. De Frutos S, Luengo A, García-Jérez A, Hatem-Vaquero M, Griera M, O'Valle F, Rodríguez-Puyol M, Rodríguez-Puyol D, Calleros L. Chronic kidney disease induced by an adenine rich diet upregulates integrin linked kinase (ILK) and its depletion prevents the disease progression. Biochim Biophys Acta Mol Basis Dis. 2019 Jun 1;1865(6):1284-1297. doi: 10.1016/j.bbadis.2019.01.024

32. Li Q, Ming Y, Jia H, Wang G. Poricoic acid A suppresses TGF-β1-induced renal fibrosis and proliferation via the PDGF-C, Smad3 and MAPK pathways. Exp Ther Med. 2021;21:289. https://doi.org/10.3892/etm.2021.9720.

33. Muñoz Abellán C, Mangold-Gehring S, Micus S, *et al*.: A Novel Model of Chronic Kidney Disease in Rats: Dietary Adenine in Combination with Unilateral Nephrectomy. Kidney Dis. 2019; 5:135-143. doi:10.1159/000495750

34. Hung T Van, Suzuki T: Dietary fermentable fibers attenuate chronic kidney disease in mice by protecting the intestinal barrier. J Nutr. 2018; 148:552-561. doi:10.1093/jn/nxy008

35. Amini Khiabani S, Asgharzadeh M, Samadi Kafil H: Chronic kidney disease and gut microbiota. Heliyon. 2023; 9:1-17. doi:10.1016/j.heliyon.2023.e18991

36. Devlin AS, Marcobal A, Dodd D, Nayfach S, Plummer N, Meyer T, *et al*. Modulation of a circulating uremic solute via rational genetic manipulation of the gut microbiota. Cell Host Microbe. 2016; 20: 709– 715. https://doi.org/10.1016/j.chom.2016.10.02 .

37. Li F, Wang M, Wang J, Li R, Zhang Y. Alterations to the Gut Microbiota and Their Correlation With Inflammatory Factors in Chronic Kidney Disease. Front Cell Infect Microbiol. 2019 Jun 12;9:206. doi: 10.3389/fcimb.2019.00206.

38. Kim, J.E.; Kim, H.E.; Park, J.I.; Cho, H.; Kwak, M.J.; Kim, B.Y.; Yang, S.H.; Lee, J.P.; Kim, D.K.; Joo, K.W.; *et al*. The Association between Gut Microbiota and Uremia of Chronic Kidney Disease. Microorganisms 2020, 8, 1-14-doi: 10.3390/microorganisms8060907.

39. Chan, W.; Bosch, J.A.; Phillips, A.C.; Chin, S.H.; Antonysunil, A.; Inston, N.; Moore, S.; Kaur, O.; McTernan, P.G.; Borrows, R. The Associations of Endotoxemia With Systemic Inflammation, Endothelial Activation, and Cardiovascular Outcome in Kidney Transplantation. J. Ren. Nutr. 2018, 28, 13–27. doi: 10.1053/j.jrn.2017.06.004

40. Lim, Y.J.; Sidor, N.A.; Tonial, N.C.; Che, A.; Urquhart, B.L. Uremic Toxins in the Progression of Chronic Kidney Disease and Cardiovascular Disease: Mechanisms and Therapeutic Targets. Toxins 2021, 13, 1-26. doi: 10.3390/toxins13020142.

41. He L, Yan X, Wen S, Zhong Z, Hou Z, Liu F, Mi H. Paris. Paris polyphylla extract attenuates colitis in mice by regulating PPAR-γ mediated Treg/Th17 balance. J Ethnopharmacol. 2023; 314:1-9. doi:10.1016/j.jep.2023.116621

42. Cheng, C., Zhang, W., Zhang, C., Ji, P., Wu, X., Sha, Z., Chen, X., Wang, Y., Chen, Y., Cheng, H., Shi, L. Hyperoside ameliorates DSS-induced colitis through MKRN1-mediated regulation of PPARgamma signaling and Th17/Treg balance. J. Agric. Food Chem. 2021. 69:, 15240–15251. doi: 10.1021/acs.jafc.1c06292

43. Wen, S., He, L., Zhong, Z., Zhao, R., Weng, S., Mi, H., Liu, F., 2021. Stigmasterol restores the balance of Treg/Th17 cells by activating the butyrate-PPARgamma Axis in colitis. Front. Immunol. 12, 741934. doi: 10.3389/fimmu.2021.741934.

44. Decara J, Rivera P, López-Gambero AJ, Serrano A, Pavón FJ, Baixeras E, Rodríguez de Fonseca F, Suárez J. Peroxisome Proliferator-Activated Receptors: Experimental Targeting for the Treatment of Inflammatory Bowel Diseases. Front Pharmacol. 2020; 11:1-18. doi:10.3389/fphar.2020.00730

45. Ji X, Su L, Zhang P, Yue Q, Zhao C, Sun X, Li K, Liu X, Zhang S, Zhao L Lentinan improves intestinal inflammation and gut dysbiosis in antibiotics-induced mice. Sci Rep. 2022; 12:1-12. doi:10.1038/s41598-022-23469-2

46. Villanacci V, Del Sordo R, Parigi TL, Leoncini G, Bassotti G: Inflammatory Bowel Diseases: Does One Histological Score Fit All? Diagnostics. 2023; 13:1-12. doi:10.3390/diagnostics13122112

47. López-Cauce B, Puerto M, García JJ, Ponce-Alonso M, Becerra-Aparicio F, Del Campo R, Peligros I, Fernández-Aceñero MJ, Gómez-Navarro Y, Lara JM, Miranda-Bautista J, Marín-Jiménez I, Bañares R, Menchén L. Akkermansia deficiency and mucin depletion are implicated in intestinal barrier dysfunction as earlier event in the development of inflammation in interleukin-10-deficient mice. Front Microbiol. 2023;13:1-19. doi: 10.3389/fmicb.2022.1083884.

48. Wang R, Hu B, Ye C, Zhang Z, Yin M, Cao Q, Ba Y, Liu H. Stewed Rhubarb Decoction Ameliorates Adenine-Induced Chronic Renal Failure in Mice by Regulating Gut Microbiota Dysbiosis. Front Pharmacol. 2022; 13:1-18. doi:10.3389/fphar.2022.842720

49. Saranya, G.R.; Viswanathan, P. Gut Microbiota Dysbiosis in AKI to CKD Transition. Biomed. Pharmacother. 2023, 161, 1-9. doi: 10.1016/j.biopha.2023.114447

50. Leon-Coria, A., Kumar, M., Workentine, M., Moreau, F., Surette, M., and Chadee, K. Muc2 mucin and nonmucin microbiota confer distinct innate host defense in disease susceptibility and colonic injury. Cell. Mol. Gastroenterol. Hepatol.2021; 11, 77–98. doi: 10.1016/j.jcmgh.2020.07.003.

51. Sasu A, Herman H, Mariasiu T, Rosu M, Balta C, Anghel N, Miutescu E, Cotoraci C, Hermenean A. Protective effects of silymarin on epirubicin-induced mucosal barrier injury of the gastrointestinal tract. Drug Chem Toxicol. 2015 ;38:442-51. doi: 10.3109/01480545.2014.992072.

52. Cheng S, Li H, Huang Y, Su Y, Li Y, Jia A, Jiang Y, Zhang Y, Man C. Lactobacillus gasseri JM1 Isolated from Infant Feces Alleviates Colitis in Mice via Protecting the Intestinal Barrier. Nutrients. 2022 28;15:139. doi: 10.3390/nu15010139

53. Deplancke B, Gaskins HR, Microbial modulation of innate defense: Goblet cells and the intestinal mucus layer. Am. J. Clin. Nutr 2001; 73: 1131S–1141S. doi: 10.1093/ajcn/73.6.1131S.

54. Suzuki T. Regulation of intestinal epithelial permeability by tight junction. Cell Mol Life Sci 2013; 70:631–59 doi: 10.1007/s00018-012-1070-x.

55. Kanbay M, Onal EM, Afsar B, Dagel T, Yerlikaya A, Covic A, *et al*. The crosstalk of gut microbiota and chronic kidney disease: role of inflammation, proteinuria, hypertension, and diabetes mellitus. Int Urol Nephrol. 2018; 50:1453–1466. doi.org/10.1007/s11255-018-1873-2

56. Huang Y, Zhou J, Wang S, Xiong J, Chen Y, Liu Y, Xiao T, Li Y, He T, Li Y, Bi X, Yang K, Han W, Qiao Y, Yu Y, Zhao J: Indoxyl sulfate induces intestinal barrier injury through IRF1-DRP1 axis-mediated mitophagy impairment. Theranostics. 2020; 10:7384-7400. doi:10.7150/thno.45455

57. Hagen SJ. Non-canonical functions of claudin proteins: Beyond the regulation of cell-cell adhesions. Tissue Barriers. 2017; 5:1-14. doi:10.1080/21688370.2017.1327839

58. Čužić S, Antolić M, Ognjenović A, Stupin-Polančec D, Petrinić Grba A, Hrvačić B, Dominis Kramarić M, Musladin S, Požgaj L, Zlatar I, Polančec D, Aralica G, Banić M, Urek M, Mijandrušić Sinčić B, Čubranić A, Glojnarić I, Bosnar M, Eraković Haber V. Claudins: Beyond Tight Junctions in Human IBD and Murine Models. Front Pharmacol. 2021; 12:1-15. doi:10.3389/fphar.2021.682614

59. Denney, L.; Byrne, A.J.; Shea, T.J.; Buckley, J.S.; Pease, J.E.; Herledan, G.M.;Walker, S.A.; Gregory, L.G.; Lloyd, C.M. Pulmonary Epithelial Cell-Derived Cytokine TGF-beta1 Is a Critical Cofactor for Enhanced Innate Lymphoid Cell Function. Immunity 2015, 43, 945–958. doi: 10.1016/j.immuni.2015.10.012

60. Bording-Jorgensen M, Armstrong H, Wickenberg M, LaPointe P, Wine E: Macrophages and Epithelial Cells Mutually Interact through NLRP3 to Clear Infection and Enhance the Gastrointestinal Barrier. Immuno. 2021; 2:13-25. doi:10.3390/immuno2010002

61. Ito F, Sono Y, Ito T: Measurement and clinical significance of lipid peroxidation as a biomarker of oxidative stress: Oxidative stress in diabetes, atherosclerosis, and chronic inflammation. Antioxidants. 2019; 8:1-28. doi:10.3390/antiox8030072

62. Sueyoshi M, Fukunaga M, Mei M, Nakajima A, Tanaka G, Murase T, Narita Y, Hirata S, Kadowaki D. Effects of lactulose on renal function and gut microbiota in adenine-induced chronic kidney disease rats. Clin Exp Nephrol. 2019; 23:908-919. doi:10.1007/s10157-019-01727-4

63. Saito H, Miyakoshi N, Kasukawa Y, Nozaka K, Tsuchie H, Sato C, Abe K, Shoji R, Shimada Y. Analysis of bone in adenine-induced chronic kidney disease model rats. Osteoporos Sarcopenia. 2021; 7:121-126. doi:10.1016/j.afos.2021.11.001

64. Yanat M, Schroën K: Preparation methods and applications of chitosan nanoparticles; with an outlook toward reinforcement of biodegradable packaging. React Funct Polym. 2021; 161:1-12. doi:10.1016/j.reactfunctpolym.2021.104849

65. Abdelgawad, A.M.; El-Naggar, M.E.; Hudson, S.M.; Rojas, O.J. Fabrication and characterization of bactericidal thiol-chitosan and chitosan iodoacetamide nanofibres. Int. J. Biol. Macromol. 2017, 94, 96–105 doi: 10.1016/j.ijbiomac.2016.07.061.

66. Zeng, Z.W.;Wang, J.J.; Xiao, R.Z.; Xie, T.; Zhou, G.L.; Zhan, X.R.;Wang, S.L. Recent advances of chitosan nanoparticles as drug carriers. Int. J. Nanomed. 2011, 6, 765–774. doi: 10.2147/IJN.S17296

67. Nomier YA, Alshahrani S, Elsabahy M, Asaad GF, Hassan A, El-Dakroury WA: Ameliorative effect of chitosan nanoparticles against carbon tetrachloride-induced nephrotoxicity in Wistar rats. Pharm Biol. 2022; 60:2134-2144. doi:10.1080/13880209.2022.2136208

68. Bai W, Wang S, An S, Guo M, Gong G, Liu W, Ma S, Li X, Fu J, Yao W Combination therapy of chitosan, gynostemma, and motherwort alleviates the progression of experimental rat chronic renal failure by inhibiting STAT1 activation. Oncotarget. 2018; 9:15498-15511. doi:10.18632/oncotarget.24125

69. Niu W, Dong Y, Fu Z, Lv J, Wang L, Zhang Z, Huo J, Ju J. Effects of molecular weight of chitosan on anti-inflammatory activity and modulation of intestinal microflora in an ulcerative colitis model. Int J Biol Macromol. 2021; 193:1927-1936. doi:10.1016/j.ijbiomac.2021.11.024

70. Zou P, Yang X, Wang J, Li Y, Yu H, Zhang Y, Liu G. Advances in characterisation and biological activities of chitosan and chitosan oligosaccharides, Food Chem. 190 (2016) 1174–1181. doi: 10.1016/j.foodchem.2015.06.076

71. Guo C, Zhang Y, Ling T, Zhao C, Li Y, Geng M, Gai S, Qi W, Luo X, Chen L, Zhang T, Wang N. Chitosan Oligosaccharides Alleviate Colitis by Regulating Intestinal Microbiota and PPARγ/SIRT1-Mediated NF-κB Pathway. Mar Drugs. 2022; 20:1-19. doi:10.3390/md20020096

72. Manoharan M, Aysha OS: Biological Synthesis of Chitosan and Its Activity in DSS Induced Colitis Rats. Int Multidiscip Educ Res. 2021; 10:14-24. https://s3-ap-southeast-1.amazonaws.com/ijmer/pdf/volume10/volume10-issue2(5)/4

73. Zhang J, Wan J, Chen D, Yu B, He J: Low-Molecular-Weight Chitosan Attenuates Lipopolysaccharide-Induced Inflammation in IPEC-J2 Cells by Inhibiting the Nuclear Factor-κB Signalling Pathway. Molecules. 2021; 26:569-583. doi: 10.3390/molecules26030569.

74. Gao BT, Lee RP, Jiang Y, Steinle JJ, Morales-Tirado VM. Pioglitazone alters monocyte populations and stimulates recent thymic emigrants in the BBDZR/Wor type 2 diabetes rat model. Diabetol Metab Syndr. 2015 ;7:1-11. doi: 10.1186/s13098-015-0068-6

75. Faiz S, Arshad S, Kamal Y, Imran S , Asim MH , Mahmood A , Inam S , Irfan HM , Riaz H. Pioglitazone-loaded nanostructured lipid carriers : In-*vitro* and in-*vivo* evaluation for improved bioavailability. J Drug Deliv Sci Technol. 2023; 79:1-8. doi:10.1016/j.jddst.2022.104041

76. Li J, Cai C, Li J, Li J, Li J, Sun T, Wang L, Wu H, Yu G. Chitosan-based nanomaterials for drug delivery, Molecules 2018;23:1-26, https://doi.org/ 10.3390/molecules23102661

77. M Ways TM, Lau WM, Khutoryanskiy VV. Khutoryanskiy, Chitosan and its derivatives for application in mucoadhesive drug delivery systems, Polymers (Basel) 2018;10:1-37, https://doi.org/10.3390/polym10030267.

78. Liu Y, Yang G, Jin S, Xu L, Zhao C xia. Development of High-Drug-Loading Nanoparticles. Chempluschem. 2020; 85:2143-2157. doi:10.1002/cplu.202000496

79. Elumalai K, Srinivasan S, Shanmugam A: Review of the efficacy of nanoparticle-based drug delivery systems for cancer treatment. Biomed Technol. 2024; 5:109-122. doi:10.1016/j.bmt.2023.09.001

80. Medić B, Stojanović M, Rovčanin B, Kekić D, Škodrić SR, Jovanović GB, Vujović KS, Divac N, Stojanović R, Radenković M, Prostran M Pioglitazone attenuates kidney injury in an experimental model of gentamicin-induced nephrotoxicity in rats. Sci Rep. 2019; 9:1-10. doi:10.1038/s41598-019-49835-1

81. Németh Á, Mózes MM, Calvier L, Hansmann G, Kökény G: The PPARγagonist pioglitazone prevents TGF-β induced renal fibrosis by repressing EGR-1 and STAT3. BMC Nephrol. 2019; 20:1-9. doi:10.1186/s12882-019-1431-x

82. Li JM, Yu R, Zhang LP, Wen SY, Wang SJ, Zhang XY, Xu Q, Kong LD. Dietary fructose-induced gut dysbiosis promotes mouse hippocampal neuroinflammation: A benefit of short-chain fatty acids. Microbiome. 2019; 7:1-15. doi:10.1186/s40168-019-0713-7

83. Da Rocha GHO, de Paula-Silva M, Broering MF, Scharf PRDS, Matsuyama LSAS, Maria-Engler SS, Farsky SHP. Pioglitazone-Mediated Attenuation of Experimental Colitis Relies on Cleaving of Annexin A1 Released by Macrophages. Front Pharmacol. 2020; 11:1-19. doi:10.3389/fphar.2020.591561

84. Al-Muzafar HM, Alshehri FS, Amin KA. The role of pioglitazone in antioxidant, anti-inflammatory, and insulin sensitivity in a high fat-carbohydrate diet-induced rat model of insulin resistance. Brazilian J Med Biol Res. 2021; 54:1-10. doi:10.1590/1414-431X2020E10782

85. Boonzaier J, Van der Merwe EL, Bennett NC, Kotzé SH. A comparative histochemical study of the distribution of mucins in the gastrointestinal tracts of three insectivorous mammals. Acta Histochem. 2013;115:549-56. doi: 10.1016/j.acthis.2012.12.003.

86. Huang Y, Wang C, Tian X, Mao Y, Hou B, Sun Y, Gu X, Ma Z. Pioglitazone Attenuates Experimental Colitis-Associated Hyperalgesia through Improving the Intestinal Barrier Dysfunction. Inflammation. 2020; 43:568-578. doi:10.1007/s10753-019-01138-3

87. Abdel-Hamed AR, Hamouda AO, Abo-elmatty DM, Khedr NF, Ghattas MH. Role of Kaempferol Combined with Pioglitazone in the Alleviation of Inflammation and Modulation of Necroptosis and Apoptosis Pathways in NASH-induced Mice. Journal of Medicinal and Chemical Sciences. 2023;6:250-268. DOI: 10.26655/JMCHEMSCI.2023.2.8

الملخص العربى

التأثير العلاجي المحتمل لجزيئات الكيتوزان المتناهية الصغر مقابل البيوجليتازون المحمل على جزيئات الكيتوزان المتناهية الصغر على إلتهاب القولون المصاحب لمرض الكلى المزمن فى نموذج ذكر الجرذ الأبيض البالغ. دراسة هستولوجية و كيميائيه حيوية

رقية محمد حسن، صافيناز صلاح الدين السيد، آلاء سراج الدين حبيب، مروة محمد يسري
قسم علم الأنسجة، كلية الطب، جامعة القاهرة، القاهرة، مصر

الخلفية: يعد التهاب القولون وإختلال التوازن البكتيري فى الأمعاء واحد من مسبباتومضاعفات مرض الكلى المزمن. بيوجليتازون هيدروكلوريد هو دواء مضاد لمرض السكر، يحفز المستقبل المنشط بمكاثر البيروكسيسوم غاما ويمتلك تأثيرات مضادة للأكسدة ومضادة للالتهابات. يؤدي انخفاض ذوبانة المائي إلى محدودية امتصاصه وديناميكيته الدوائية. لذلك، يعد نظام توصيل الدواء عن طريق الجزيئات المتناهية الصغر أولوية.
هدف العمل: تقييم التأثير العلاجي المحتمل لجزيئات الكيتوزان المتناهية الصغر مقابل البيوجليتازون هيدروكلوريدالمحمل على جزيئات الكيتوزان المتناهية الصغرعلى إلتهاب القولون المصاحب لمرض الكلى المزمن.
المواد وطرق البحث: تم تقسيم تسعة وعشرين من ذكور الجرذان البالغة إلى خمس مجموعات المجموعة الأولى ، المجموعة الثانية التى تلقت أدينين يوميا لمدة ثلاثة أسابيع، المجموعة الثالثة عولجت، كما بالمجموعة الثانية ثم تركت بدون أي تدخل أخر لمدة إسبوعين المجموعتين الرابعة والخامسة تلقوا أدينين كما بالمجموعة الثانية ثمجزيئات الكيتوزان المتناهية الصغر او بيوجليتازون المحمل على جزيئات الكيتوزان المتناهية الصغر على التوالي لمدة إسبوعين. تم إجراء التحاليل الكيميائية الحيوية للعصية اللبنية في البراز ونسبة الكرياتينين في مصل الدم ومالونديالدهيد وعامل نخر الورم ألفا ومستقبل منشط بمكاثر البيروكسيسوم غاما فى القولون. وايضا تمإجراء الدراسات الهستولوجية والهستوكيميائية المناعية- ضد كلودين ١- وكاسبيز ٣ بالاضافة الى دراسات إحصائية.
النتائج: أوضحت المجموعة الثانية ارتفاع الكرياتينين في الدم ومالونديالدهيد وعامل نخر الورم ألفا فى القولون بالإضافة إلى انخفاض تعبير العصيات اللبنية في البراز ومستقبل منشط بمكاثر البيروكسيسوم غاما . تم تسجيل إضطراب في بنية الكلية مع فقدان النسيج الطلائي لسطح القولون وتشوه الجريب المعوى وتخلل التهابي. بالإضافة إلى انخفاض الكلودين -١ وزيادة النشاط المناعي للكاسبيز -٣. فيما يخص المجموعة الثالثة فلم تسجل أي تحسن ملحوظ في جميع النتائج التى ذكرت سابقا. بينما أظهرت المجموعة الرابعة والخامسة تحسنا واضحا مع تأثيرات أفضل في المجموعة الخامسة.
الاستنتاج: حسن كلا من جزيئات الكيتوزان المتناهية الصغر والبيوجليتازون المحمل على جزيئات الكيتوزان المتناهية الصغر تغيرات وظيفة وبنية الكلية ،كما حسنوا التهاب القولون المصاحب لمرض الكلى المزمن. بينما اظهر البيوجليتازون المحمل على جزيئات الكيتوزان المتناهية الصغر تاثيرات فائقة.